FEATURE EXTRACTION AND IDENTIFICATION TECHNIQUES FOR THE ALIGNMENT OF PERTURBATION SIMULATIONS WITH POWER PLANT MEASUREMENTS

George Ioannou[1], Thanos Tasakos[1], Antonios Mylonakis[2], Georgios Alexandridis[1], Christophe Demaziere[2], Paolo Vinai[2], and Andreas Stafylopatis[1]

[1]School of Electrical & Computer Engineering
National Technical University of Athens
Zografou, 157 80, Greece

[2]Chalmers University of Technology
Department of Physics
Division of Subatomic, High Energy and Plasma Physics
SE-412 96 Gothenburg, Sweden

geoioannou@islab.ntua.gr, thanostas@islab.ntua.gr, antonios.mylonakis@chalmers.se, gealexandri@islab.ntua.gr, demaz@chalmers.se, vinai@chalmers.se, andreas@cs.ntua.gr

dx.doi.org/10.13182/M&C21-33674

ABSTRACT

In this work, a methodology is proposed for the comparison of the measured and simulated neutron noise signals in nuclear power plants, with the simulation sets having been generated by the CORE SIM+ diffusion-based reactor noise simulator. More specifically, the method relies on the computation of the Cross-Power Spectral Density of the detector signals and the subsequent comparison with their simulated counterparts, which involves specific frequency values corresponding to the signals' high energy content. The different simulated perturbations considered are (i) axially traveling perturbations, (ii) fuel assembly vibrations, (iii) core barrel vibrations, and finally (iv) generic "absorber of variable strength" types. The reactor core used for the current study is a German 4-loop pre-Konvoi Pressurized Water Reactor.

KEYWORDS: neutron noise, cross-power spectral density, feature extraction, perturbation identification, simulation, core diagnostics, CORE SIM+

1. INTRODUCTION

Due to the aging fleet of nuclear reactors in Europe and worldwide, core monitoring and diagnostics techniques are becoming increasingly essential for performance and public safety [1]. Although many works based both on signal processing and machine learning techniques exist in literature for detecting and possibly characterizing anomalies, an inherent problem that still remains is the absence of labeled perturbation measurements from the reactor cores, i.e. the actual perturbations existing in operating reactors are seldom known. In order to support the identification of possible anomalies, reactor core simulation packages and solvers have been developed, for which the response of the reactors is estimated assuming various postulated anomalies [2,3].

In previous studies [4,5], the effectiveness of Deep Learning architectures for perturbation localization and identification has been demonstrated. After reviewing the relevant literature in Section 2, an alternative approach is considered in this work, where the focus is shifted to feature extraction for the assessment of the core state. The simulated data consist of examples of perturbations produced by the CORE SIM+ simulation software [6], which are further described in Section 3. The proposed methodology is outlined in Section 4, the results are discussed in Section 5 and the conclusions are summarized in Section 6.

2. RELATED WORK

Signal processing algorithms based on simulations and real measurements have been developed and applied to assess the core state of a nuclear power plant and diagnose possible anomalies. In recent years various works have been published utilizing Machine Learning models in order to classify any perturbations occurring inside the core. For example, Symbolic Dynamic Filtering has been utilized to down-sample the input detector signals and then train a classifier [7], resulting in performance improvement over Principal Component Analysis (PCA) on simulated data produced with the International Reactor Innovative & Secure (IRIS) simulator. Other approaches utilize Support Vector Machines (SVMs) in order to assess the state of the reactor core [8] or in outlier identification on neutron flux signals originating from a nuclear reactor channel [9]. It should be mentioned that those past studies do not consider the neutron noise as input data, with the noise defined as the deviation of the signal from its mean value. Rather, the total response is analyzed.

Turning to the analysis of the neutron noise, deep learning techniques based on neural network architectures have recently been considered for diagnostics. In [10], a hybrid system consisting of a Convolutional Neural Network (CNN) and a Denoising Autoencoder (DAE), followed by the k-means clustering algorithm has been proposed for perturbation identification and localization. The experiments performed with the neutron noise simulator CORE SIM [2] exhibited satisfactory classification accuracy, even in the presence of additive noise in the signals, indicating the robustness of the proposed approach. For improved localization of perturbations, a 3-dimensional CNN architecture has been employed in [11], for the processing of data in the frequency domain. In the same work, data produced by the SIMULATE-3K code [3] in the time-domain have been processed by a Long Short-Term Memory (LSTM) network.

The utilization of the wavelet transformation of detector signals in a CNN architecture for efficient perturbation classification has been proposed in [4]. Similarly, an ensemble of neural networks constituted of 1-dimensional convolutions that extracts the spatial characteristics of the detrended neutron detector signals, followed by LSTM layers that capture temporal features of the signals, has been outlined in [5]. Each neural network has been trained to identify one specific perturbation type, with the experimental results showing a combined identification accuracy of over 80%.

3. NEUTRON NOISE SIGNALS

3.1. Simulated data

The simulations of the neutron noise induced by various types of perturbations were performed in the frequency-domain using the CORE SIM+ tool [6]. This tool estimates the effect of stationary

perturbations in macroscopic cross-sections onto the neutron flux using the two-group diffusion approximation, in linear theory and assuming one group of delayed neutrons. The spatial discretization of the balance equations is based on finite differences in Cartesian geometry. Depending on the problem of interest, different numerical methods and non-uniform computational meshes can be selected for effective numerical performance and accuracy. Several anomalies were considered and the associated neutron noise was estimated, i.e.:

1. Axially traveling perturbations at the velocity of the coolant flow, where a perturbation is created at some spatial location in the core and travels upwards with the flow through the core. All possible locations of the perturbation were considered for frequencies ranging from 0.1 to 25 Hz.
2. Fuel assembly vibrations, for which the lateral movement of fuel assemblies was modeled according to the following modes of vibrations: the cantilevered beam mode (for frequencies ranging from 0.6 to 1.2 Hz), the simply supported on both sides mode (with its two first harmonics - frequencies ranging from 0.8 to 4.0 Hz for the first mode and frequencies ranging from 5.0 to 10.0 Hz for the second mode), and the cantilevered beam and simply supported mode (with its two first harmonics - frequencies ranging from 0.8 to 4.0 Hz for the first mode and frequencies ranging from 5.0 to 10.0 Hz for the second mode). All possible locations of the vibrating fuel assembly were modeled.
3. Core barrel vibrations, where the core barrel was assumed to vibrate in the beam or pendular mode for frequencies ranging from 7 to 13 Hz.
4. Generic "absorber of variable strength", where a spatial Dirac-like perturbation is assumed. All possible locations of the perturbation were considered for frequencies ranging from 0.1 to 25 Hz.

The modeling of the corresponding noise source for the above scenarios is described in detail in [12,13]. From the spatial dependence of the induced neutron noise estimated by CORE SIM+, the Cross-Power Spectral Densities (CPSD) of the relative neutron noise (compared to the static neutron flux) between pairs of neutron detectors were calculated. The underlying reason for calculating the CPSD was to ensure consistency between the simulations and the type of quantities determined from the analysis of the measured plant data.

3.2. Plant Measurements

The plant measurements used in this work originate from a German 4-loop Pressurized Water Reactor (PWR) [14,15]. Figure 1 displays a cross-section of the aforementioned reactor, where the fuel assemblies and its detectors are visible. In total, three different types of detectors are present; (i) in-core neutron detectors, denoted by L, (ii) thermal detectors, denoted by T (both in green color), (iii) ex-core neutron detectors, denoted by X (in pink color) and (iv) pressure sensors, denoted by P (in blue color). The in-core neutron detectors lie at 6 distinct axial levels (hence the 1/6 notation in Figure 1), while the ex-core neutron detectors lie at 2 distinct axial levels.

In this study, only the sensors that measure neutron noise (in-core & ex-core) are considered. The signals are captured in the time domain, their length is around 30 minutes and the sampling rate is

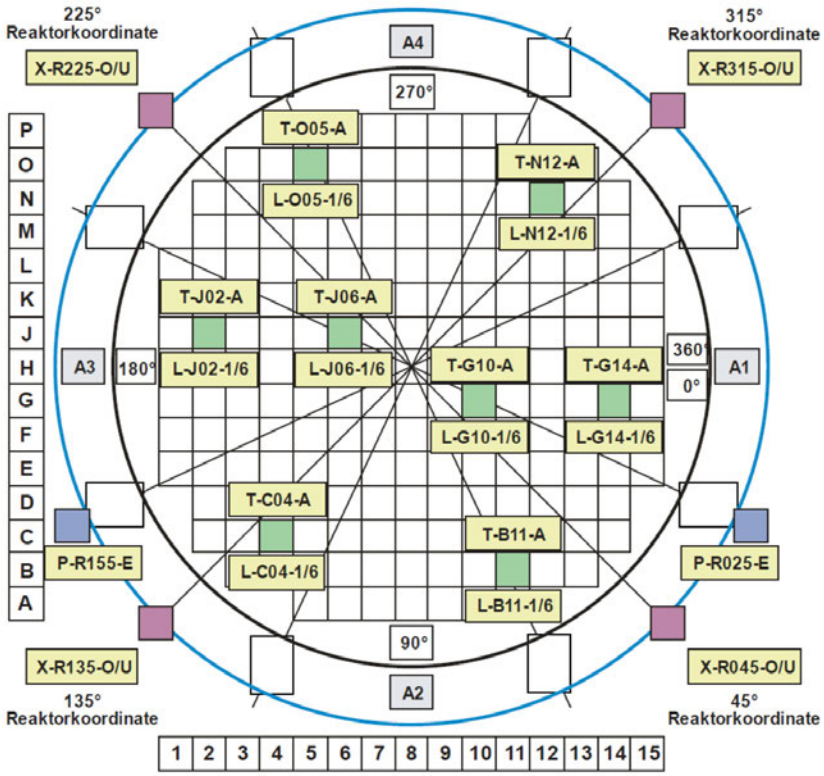

Figure 1: A cross-section of the core of the German 4-loop PWR [14,15]

$250Hz$, resulting in $450,560$ discrete time samples. Some of the detectors were known to exhibit faulty behavior, so they were disregarded. In total 53 sensors have been considered, 45 in-core and 8 ex-core. As a first pre-processing step, the Direct Current (DC) component has been removed from all signals (Figure 2). Subsequently, all signals were checked for the existence of trend; in some cases, a small trend was still present and was removed by a linear detrending algorithm. The whole process is outlined in Figure 2 for the in-core detector B11 at axial level 3 (L-B11-3).

4. PROPOSED METHODOLOGY

The aim of the proposed methodology is to find and align frequency regions in Nuclear Power Plant (NPP) measurements to simulated perturbations. In this way, it is possible to identify which perturbations are more likely occurring within the core and at the same time predict their source. The overall approach is comprised of two steps; initially, the frequency peaks of the Auto-Power Spectral Densities (APSDs) of the plant measurements are determined. These peaks constitute the candidate frequencies of a possible perturbation. Then the CPSDs between the detector signals are computed for each of the candidate frequencies. These CPSDs are compared with the CPSDs evaluated from the neutron noise simulated with CORE SIM+ for each of the perturbations described in Section 3.1. These comparisons quantify the degree of similarity between measurements and simulated scenarios and thus can indicate the possible type and location of the occurring perturbations. The specifics of the approach will be described in more detail in the following subsections.

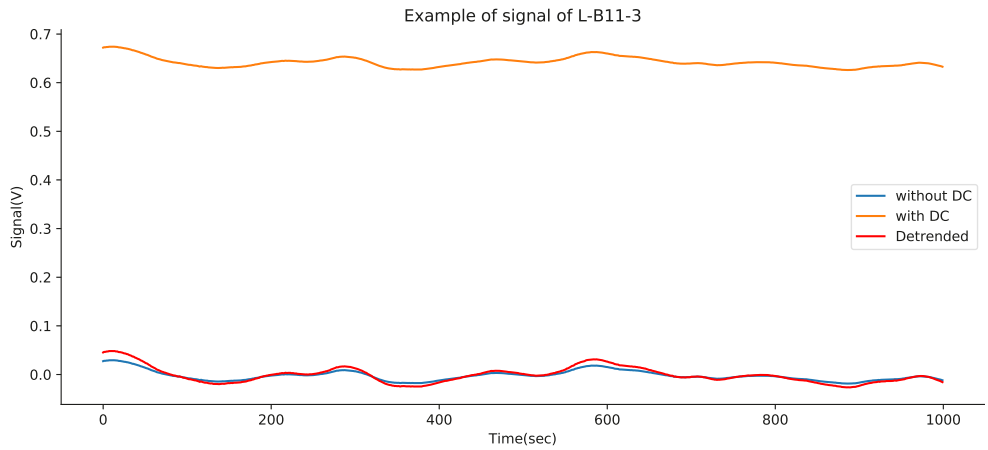

Figure 2: Detrending in-core signal L-B11-3; (i) original signal (orange line), (ii) signal without the DC component (blue line) and (iii) signal without the DC component & the linear trend (red line)

4.1. Determining the frequency peaks

In order to identify crucial frequencies corresponding to possible perturbations, the APSDs of all plant measured signals are calculated. Figure 3 displays the APSDs of all the 53 detectors, computed using Welch's algorithm [16] and grouped by position.

As evident in Figure 3, each group of sensors usually exhibits the same frequency peaks. To select the candidate frequencies for our analysis, a voting scheme has been employed, where the frequencies considered appear in the majority of sensor groups as peaks in the APSD. Eq. 1 summarizes the candidate frequency set

$$\{0.3Hz, 0.7Hz, 1Hz, 6Hz, 10Hz, 13Hz, 15Hz, 20Hz, 23Hz\} \tag{1}$$

4.2. Computing the similarities

The CPSDs of all the detector signals are computed for each of the candidate frequencies . In addition, CPSDs are evaluated from the neutron noise calculated for each of the perturbations described in Section 3.1 (which are of different types, at different frequencies and in different locations). The CPSDs of the plant data, being in time domain, are extracted by the Welch's algorithm (just like the APSDs). The simulations performed with CORE SIM+ are in the frequency domain, so the CPSD of the relative neutron noise ($\frac{\delta\phi}{\phi_0}$) between detectors i, j is calculated according to Eq. 2

$$CPSD_{i,j} = \left(\frac{\delta\phi}{\phi_0}\right)_i \left(\frac{\delta\phi}{\phi_0}\right)_j^{\dagger} \tag{2}$$

where † symbolizes the complex conjugate.

As a result, since the number of detectors is 53, 53×53 matrices of CPSDs are created. On one hand, a set of matrices is obtained from the measurements, for each of the candidate frequencies.

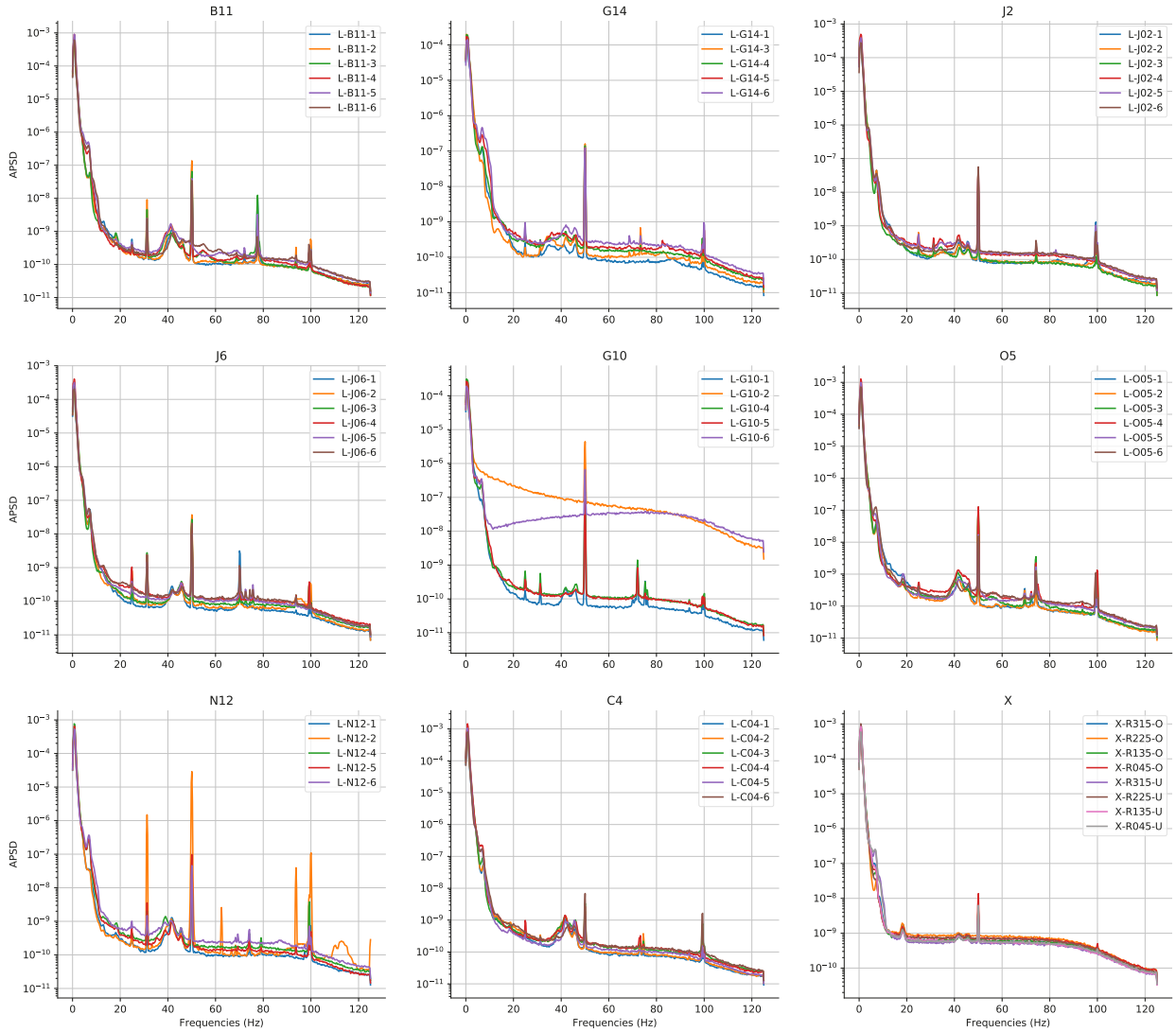

Figure 3: APSDs of all the detectors grouped by their position in the grid

On the other hand, a set of matrices is build from each of the simulated neutron noise scenarios (which differ because of perturbation type, location and frequency). In order to quantify how similar one of the matrices based on the measurements is to one of the matrices based on the simulations, a relevant measure from the literature is employed, namely *cosine similarity*. In the simulations, the reactor core is radially discretized according to a 34×34 grid, so the perturbations may be radially located in any of the positions identified by such a grid. Then a similarity matrix of the same size is constructed for each perturbation type & frequency. These similarity matrices can be further utilized as features by more complex machine learning algorithms for perturbation identification & localization.

In an effort to better illustrate the similarity values, heatmaps were created that capture the grid topology. More specifically, each colored square in the heatmap represents the similarity of the

plant data with a simulated perturbation originating in these exact coordinates, for a specific frequency. The whole process is summarized in Figure 4.

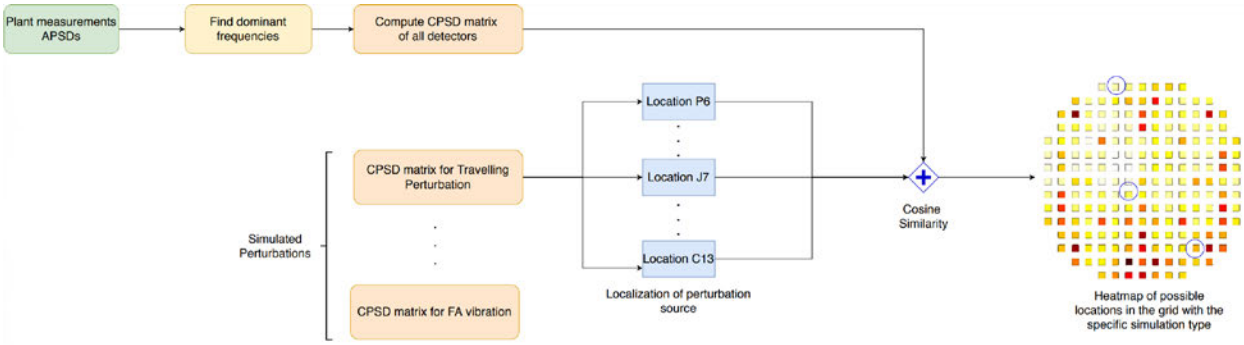

Figure 4: Proposed pipeline for the comparison of real measurements and simulated perturbation types

5. RESULTS

In this section, the obtained results of the methodology outlined in Section 4 are presented, for the simulated perturbation categories discussed in Section 3.

Axially Traveling Perturbations (ATPs): In this case, all candidate frequencies (Eq. 1) have been considered, with the highest similarity values being observed at $0.3Hz$ and $0.7Hz$ (Figure 5). At $0.3Hz$ the maximum similarity value was 0.774, located at $(13, 15)$, while at $0.7Hz$ the corresponding value was 0.681, located at the same coordinates.

Fuel Assembly Vibrations (FAVs): Since these types of perturbations exist in lower frequency ranges, only a subset of the frequencies of Eq. 1 have been examined. The highest similarity values (Figure 6) have been observed at $0.7Hz$ & $1Hz$ for the cantilevered beam mode (0.724 & 0.767, respectively, both located at $(9, 11)$) and at $1Hz$ for the cantilevered beam with supported first mode & the simply supported first mode (0.778 & 0.762, respectively, both located at $(15, 15)$).

Core Barrel Vibrations (CBVs): This perturbation type does not occur at a specific location in the core, therefore there is no need for a heatmap. The frequencies examined were $10Hz$ & $13Hz$. For both of them, the obtained similarity values were very low (around 0.155 & 0.02, respectively). This constitutes an indication that CBV were not occurring at the reactor, for the frequencies considered and at the time the neutron noise signals were captured.

Generic "Absorber of Variable Length" (AVL): AVL is the final perturbation type to be examined, serving as a form of evaluation for the other perturbation types discussed above. In fact, the

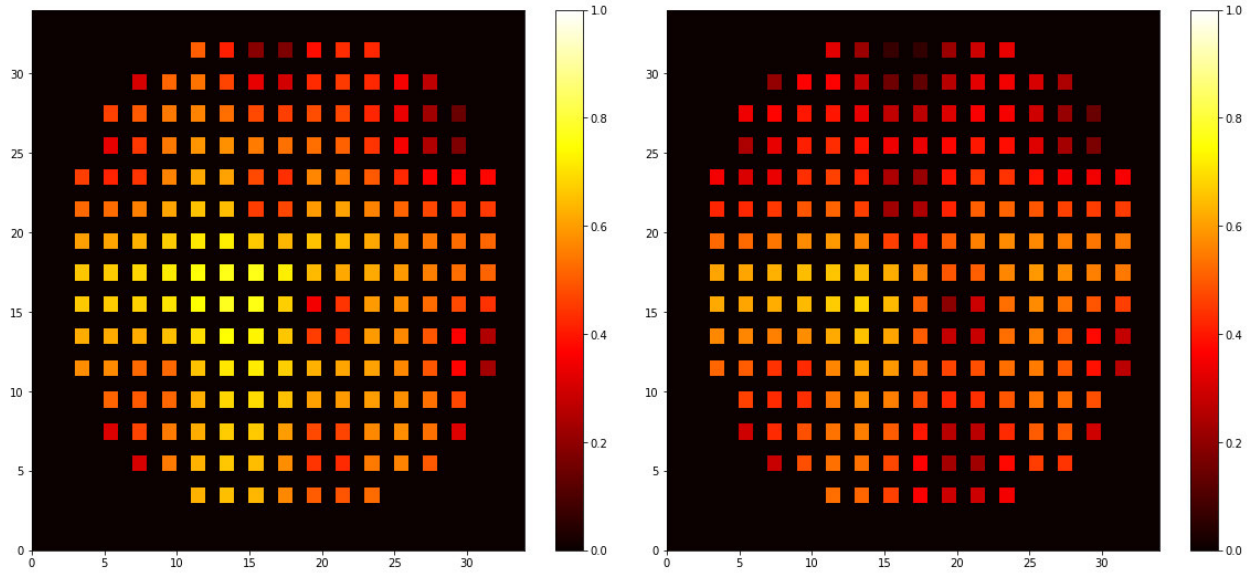

Figure 5: Similarity heatmaps of ATPs for (a) 0.3Hz and (b) 0.7Hz

absorber of variable strength is a basic perturbation that can be used to model any of the other neutron noise sources. More specifically, if comparable similarity values are computed for the same frequency & location between AVL and the other perturbation types, then this is an indication that a particular perturbation is actually occurring.

Figure 7 displays some of the heatmaps that were constructed from the similarities values of AVL perturbations and the plant measurements. The upper row depicts the heatmaps for $0.3Hz, 0.7Hz$ and $1Hz$, respectively. The maximum similarity was located at $(14, 16)$ and this position matches the previous cases of ATPs and FAVs. Therefore, it could be argued that these specific perturbations are indeed taking place at these exact frequencies & locations, which is an important conclusion, as the specific perturbations occurring within the core are, in principle, not known.

Additionally, the bottom row of Figure 7 identifies a small area in the grid around $(16, 23)$ with a very similar spatial peak at $15Hz, 20Hz$ and $23Hz$. This might indicate the existence of a perturbation type not included in the current analysis.

6. CONCLUSIONS

An attempt to draw insights into NPP measurements based on simulated perturbations has been proposed in this work. The extracted features can be either used as strong indicators for the existence of certain perturbations in the reactor core or as additional input to more advanced machine learning models that further classify and locate possible perturbations. Various similarities between known perturbation types have been identified, at specific frequencies within a German pre-Konvoi pressurized water reactor. These similarities were further validated via an analysis based on a basic perturbation such as the absorber of variable strength.

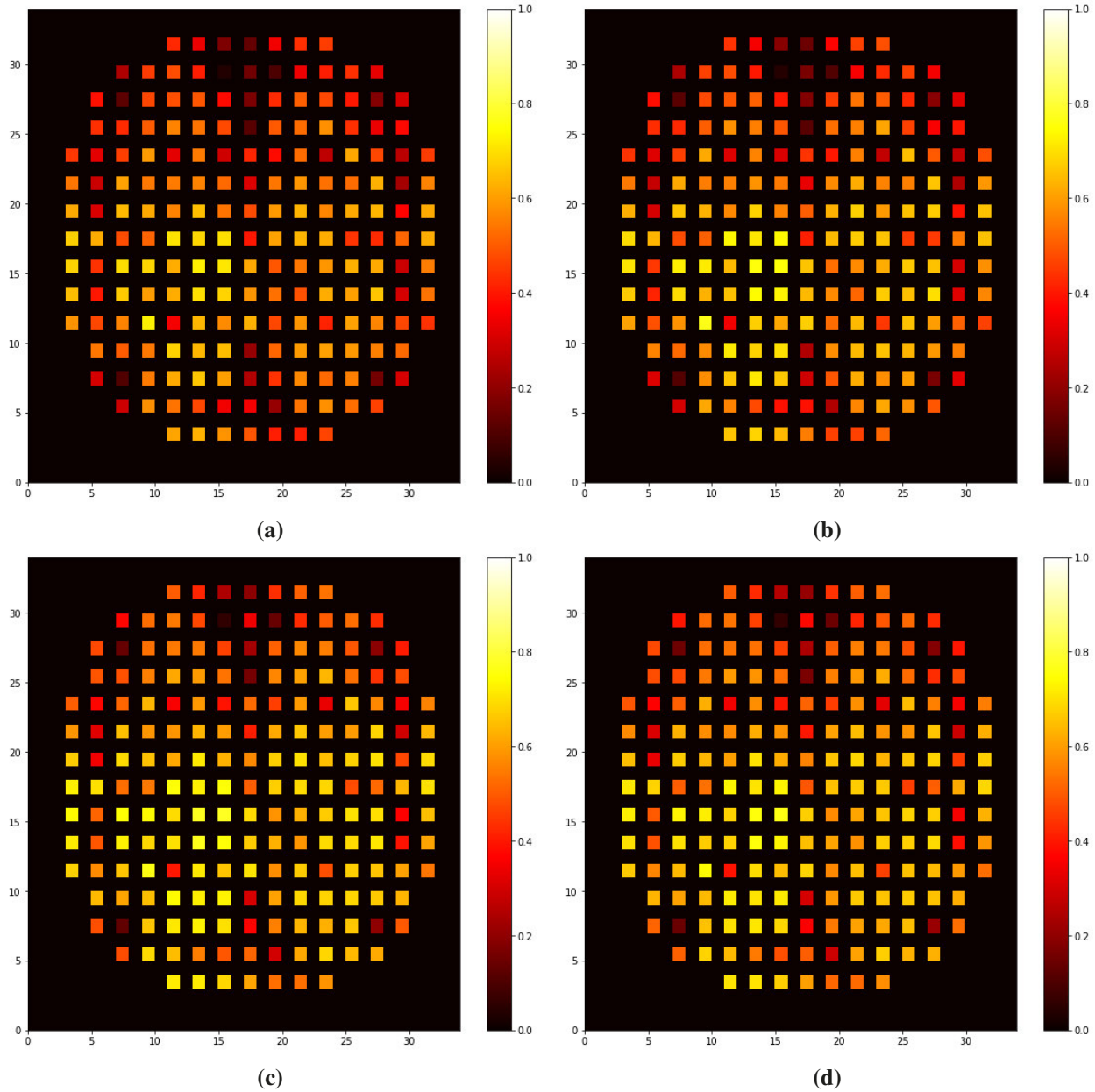

Figure 6: Similarity heatmaps of FAVs for (a) 0.7Hz cantilevered beam mode, (b) 1Hz cantilevered beam mode, (c) 1Hz cantilevered beam with supported first mode and (d) 1Hz supported first mode

For example, the same reactor with the same detectors and measurements is studied in [17], albeit a different methodology is followed. Nevertheless, both papers agree that, with a high probability, an ATP is occurring in the reactor, around grid position $(13, 15)$. Because of the lack of knowledge about which perturbations are actually taking place inside the core, a cross-verification between the different approaches would be quite useful.

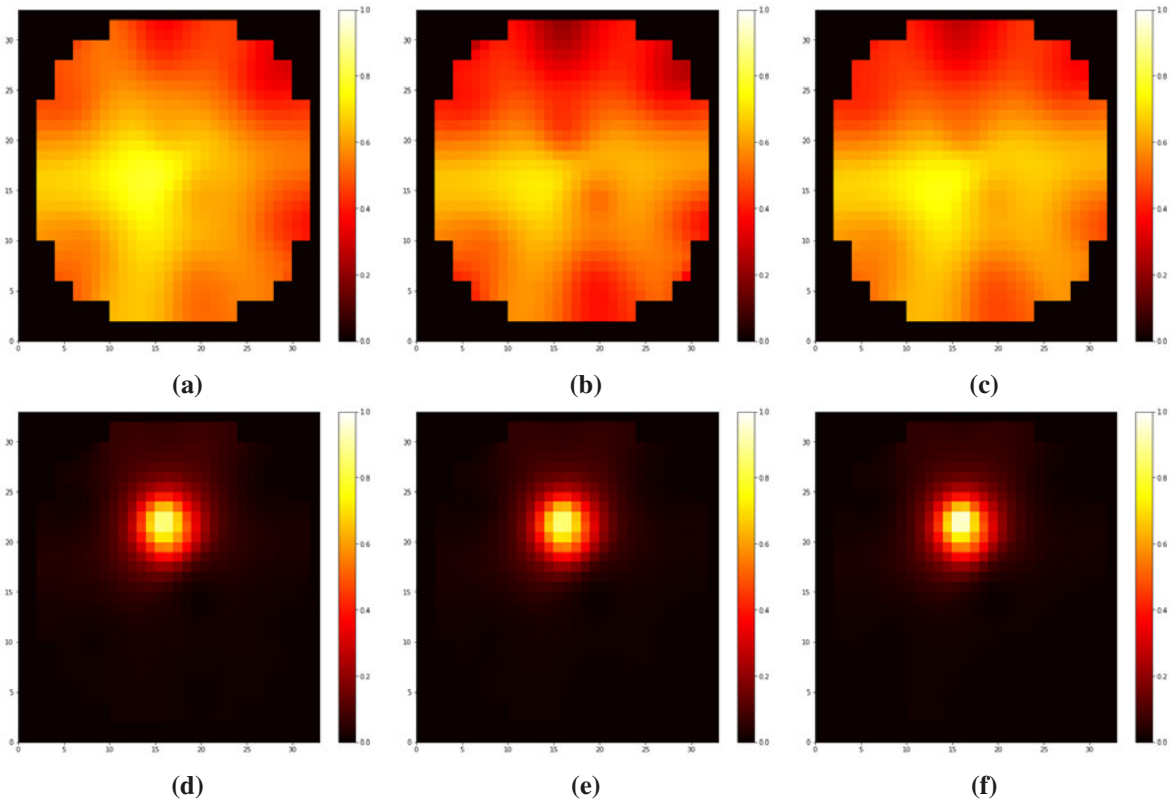

Figure 7: Similarity heatmaps of AVL for (a) 0.3Hz at axial level 18, (b) 0.7Hz at axial level 19, (c) 1Hz at axial level 18, (d) 15Hz at axial level 9, (e) 20Hz at axial level 9, (f) 23Hz at axial level 9

Finally, this work assumes that only one perturbation occurs at a specific location in the core (or, equivalently, several perturbations all having the same amplitude & phase). Therefore, an interesting extension to the current approach would be to consider multiple perturbations taking place at different amplitudes and/or phases relative to each other.

ACKNOWLEDGEMENTS

The research conducted has been made possible through funding from the Euratom research and training programme 2014-2018 under grant agreement No 754316 for the "CORe Monitoring Techniques And EXperimental Validation And Demonstration (CORTEX)" Horizon 2020 project, 2017-2021. Additionally, the authors would like to thank Preussen Elektra GmbH and Gesellschaft für Anlagen und Reaktorsicherheit GmbH for the provided actual plant measurements.

REFERENCES

[1] J. Ma and J. Jiang. "Applications of fault detection and diagnosis methods in nuclear power plants: A review." *Progress in Nuclear Energy*, **volume 53**(3), pp. 255 – 266 (2011). URL http://www.sciencedirect.com/science/article/pii/S0149197010001769.

[2] C. Demaziere. "CORE SIM: A multi-purpose neutronic tool for research and education." *Annals of Nuclear Energy*, **volume 38**(12), pp. 2698–2718 (2011).

[3] G. Grandi. "SIMULATE-3K Models & Methodology." Technical report, (SSP-98/13 Rev. 7) (2011).

[4] T. Tagaris, G. Ioannou, M. Sdraka, G. Alexandridis, and A. Stafylopatis. "Putting Together Wavelet-Based Scaleograms and Convolutional Neural Networks for Anomaly Detection in Nuclear Reactors." In *Proceedings of the 2019 3rd International Conference on Advances in Artificial Intelligence*, ICAAI 2019, p. 237–243. Association for Computing Machinery, New York, NY, USA (2019). URL https://doi.org/10.1145/3369114.3369121.

[5] G. Ioannou, T. Tagaris, G. Alexandridis, and A. Stafylopatis. "Intelligent Techniques for Anomaly Detection in Nuclear Reactors." In *Proceedings of International Conference on Physics of Reactors (PHYSOR 2020: Transition to a Scalable Nuclear Future), Cambridge, UK, March 29th - April 2nd, 2020* (2020).

[6] A. Mylonakis, P. Vinai, and C. Demazière. "CORE SIM+: A flexible diffusion-based solver for neutron noise simulations." *Annals of Nuclear Energy*, **volume 155**, p. 108149 (2021). URL https://www.sciencedirect.com/science/article/pii/S0306454921000256.

[7] X. Jin, Y. Guo, S. Sarkar, A. Ray, and R. M. Edwards. "Anomaly Detection in Nuclear Power Plants via Symbolic Dynamic Filtering." *IEEE Transactions on Nuclear Science*, **volume 58**(1), pp. 277–288 (2011).

[8] N. Zavaljevski and K. C. Gross. "Support vector machines for nuclear reactor state estimation." Technical report, Argonne National Lab. (2000).

[9] C. K. Maurya and D. Toshniwal. "Anomaly detection in nuclear power plant data using support vector data description." In *Proceedings of the 2014 IEEE Students' Technology Symposium*, pp. 82–86. IEEE (2014).

[10] F. Caliva, F. S. De Ribeiro, A. Mylonakis, C. Demaziere, P. Vinai, G. Leontidis, and S. Kollias. "A deep learning approach to anomaly detection in nuclear reactors." In *2018 International Joint Conference on Neural Networks (IJCNN)*, pp. 1–8. IEEE (2018).

[11] A. Durrant, G. Leontidis, and S. Kollias. "3D convolutional and recurrent neural networks for reactor perturbation unfolding and anomaly detection." *EPJ Nuclear Sciences & Technologies* (2019).

[12] C. Demaziere and A. Dokhane. "Cortex Deliverable D3.1: Description of scenarios for the simulated data." deliverable D3.1, Core monitoring techniques and experimental validation and demonstration (CORTEX), Horizon 2020 EU Framework Programm (No. 754316) (2019).

[13] C. Demazière, A. Mylonakis, P. Vinai, A. Durrant, F. D. S. Ribeiro, J. A. Wingate, G. Leontidis, and S. Kollias. "Neutron Noise-based Anomaly Classification and Localization using Machine Learning." In *Proceedings of International Conference on Physics of Reactors (PHYSOR 2020: Transition to a Scalable Nuclear Future), Cambridge, UK, March 29th - April 2nd, 2020* (2020).

[14] M. Kuentzel, P. Stulik, M. Seidl, S. Lipcsei, G. Girardin, and B. Schumaker. "CORTEX Deliverable 4.2: Core data for steady state calculations." deliverable D4.2, Core monitoring techniques and experimental validation and demonstration (CORTEX), Horizon 2020 EU Framework Programm (No. 754316) (2018).

[15] S. Lipcsei, S. Kiss, J. Pohlus, U. Paquee, G. Girardin, C. Pohl, M. Seidl, P. Stulik, M. Bem, J. Machek, B. Shumaker, and E. Riggsbee. "CORTEX Deliverable 4.3: Document describing

all validation data." deliverable D4.3, Core monitoring techniques and experimental validation and demonstration (CORTEX), Horizon 2020 EU Framework Programm (No. 754316) (2018).

[16] P. Welch. "The use of fast Fourier transform for the estimation of power spectra: A method based on time averaging over short, modified periodograms." *IEEE Transactions on Audio and Electroacoustics*, **volume 15**(2), pp. 70–73 (1967).

[17] A. Durrant, G. Leontidis, S. Kollias, L. A. Torres, C. Montalvo, A. Mylonakis, C. Demaziere, and P. Vinai. "DETECTION AND LOCALISATION OF MULTIPLE IN-CORE PERTURBATIONS WITH NEUTRON NOISE-BASED SELF-SUPERVISED DOMAIN ADAPTATION." In *M&C 2021 (The International Conference on Mathematics and Computational Methods applied to Nuclear Science and Engineering)*. American Nuclear Society (2021).